

University of Mississippi

eGrove

Faculty and Student Publications

Chemistry and Biochemistry

4-1-2021

Anodic Dissolution of Copper in the Acidic and Basic Aluminum Chloride 1-Ethyl-3-methylimidazolium Chloride Ionic Liquid

Lorlyn Reidy

University of Mississippi

Chen Wang

University of Mississippi

Charles L. Hussey

University of Mississippi

Follow this and additional works at: https://egrove.olemiss.edu/chem_facpubs

 Part of the [Chemistry Commons](#)

Recommended Citation

Reidy, L., Wang, C., & Hussey, C. L. (2021). Anodic dissolution of copper in the acidic and basic aluminum chloride 1-ethyl-3-methylimidazolium chloride ionic liquid. *Journal of The Electrochemical Society*, 168(4), 046503. <https://doi.org/10.1149/1945-7111/abebfa>

This Article is brought to you for free and open access by the Chemistry and Biochemistry at eGrove. It has been accepted for inclusion in Faculty and Student Publications by an authorized administrator of eGrove. For more information, please contact egrove@olemiss.edu.

OPEN ACCESS

Anodic Dissolution of Copper in the Acidic and Basic Aluminum Chloride 1-Ethyl-3-methylimidazolium Chloride Ionic Liquid

To cite this article: Lorlyn Reidy *et al* 2021 *J. Electrochem. Soc.* **168** 046503

View the [article online](#) for updates and enhancements.

You may also like

- [Template-Free Electrodeposition of Net-Like Co-Al/Oxide Structures from a Lewis Acidic Chloroaluminate Room Temperature Ionic Liquid Using a Potential Step Method](#)
Jing-Ding Fong, Po-Yu Chen and I-Wen Sun
- [Electrodeposition of Al-W-Mn Alloy from Lewis Acidic AlCl₃-1-Ethyl-3-Methylimidazolium Chloride Ionic Liquid](#)
Tetsuya Tsuda, Yuichi Ikeda, Susumu Kuwabata *et al.*
- [Aluminium Deposition in EMImCl-AlCl₃ Ionic Liquid and Ionogel for Improved Aluminium Batteries](#)
T. Schoetz, O. Leung, C. Ponce de Leon *et al.*

Investigate your battery materials under defined force!
The new PAT-Cell-Force, especially suitable for solid-state electrolytes!



- Battery test cell for force adjustment and measurement, 0 to 1500 Newton (0-5.9 MPa at 18mm electrode diameter)
- Additional monitoring of gas pressure and temperature


www.el-cell.com +49 (0) 40 79012 737 sales@el-cell.com

EL-CELL[®]
electrochemical test equipment





Anodic Dissolution of Copper in the Acidic and Basic Aluminum Chloride 1-Ethyl-3-methylimidazolium Chloride Ionic Liquid

Lorlyn Reidy,* Chen Wang,* and Charles L. Hussey**^z 

Department of Chemistry and Biochemistry, The University of Mississippi, Mississippi 38677, United States of America

The anodic dissolution of copper was investigated at a copper RDE in the Lewis acidic and basic composition regions of the room-temperature AlCl₃-EtMeImCl ionic liquid (IL) to assess the utility of chloroaluminate liquids as solvents for the electrochemical machining and electropolishing of copper. In the Lewis acidic IL (60 mol % AlCl₃), the dissolution of Cu⁰ proceeds under mixed kinetic-mass transport control with an exchange current density of 7.00 mA cm⁻² at 306 K and an apparent activation free energy of 19.7 kJ mol⁻¹. A formal potential of 0.843 V was obtained for the Cu⁺/Cu⁰ reaction from potentiometric measurements. In the basic IL (< 50 mol % AlCl₃), potentiometric measurements showed that the oxidation of Cu⁰ resulted in the formation of [CuCl₂]⁻. In this case, the formal potential of the [CuCl₂]⁻/Cu⁰ reaction is -0.412 V. At small positive overpotentials, the reaction exhibited mixed control and was first order in the chloride concentration, indicating that only a single Cl⁻ is involved in the RDS. However, at more positive overpotentials, the reaction transitions to mass transport control, and a well-defined limiting current is observed for the anodization process. This limiting current scales linearly with the free chloride concentration in the IL.

© 2021 The Author(s). Published on behalf of The Electrochemical Society by IOP Publishing Limited. This is an open access article distributed under the terms of the Creative Commons Attribution 4.0 License (CC BY, <http://creativecommons.org/licenses/by/4.0/>), which permits unrestricted reuse of the work in any medium, provided the original work is properly cited. [DOI: 10.1149/1945-7111/abefaj]



Manuscript submitted December 29, 2020; revised manuscript received March 1, 2021. Published April 9, 2021. *This paper is part of the JES Focus Issue on Molten Salts and Ionic Liquids II.*

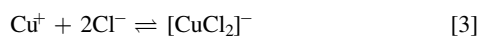
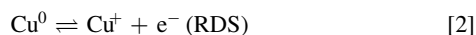
Copper is a soft, malleable metal with high thermal and electrical conductivities. Its many applications are ubiquitous in modern civilization, and it has many important applications in the manufacturing and electronics industries. It is a constituent of several important metal alloys, e.g., brass and bronze, which are used in industrial bearings and construction hardware exposed to corrosive environments, such as seawater.¹ Most importantly, copper is the material of choice for chip metallization and the fabrication of interconnects in microchips and integrated circuits.² Methods for the electrochemical processing of copper are crucial to the advancement of the microelectronics/semiconductor industry. For example, these methods include electroplating³ and those processes that involve the anodic dissolution of copper such as electrochemical machining (ECM), electrochemical-mechanical polishing^{4,5} and classical electropolishing.⁶⁻⁹

The preponderance of the methods used for the electrochemical processing of copper are based on aqueous chloride-containing solutions. This is especially true for the anodic dissolution of copper, which is the subject of this communication. Numerous investigations describing the anodic dissolution of copper in such solutions have been reported and are nicely summarized by Walsh, et al.¹⁰ Three mechanisms, more or less, have been proposed for the dissolution of copper in aqueous chloride solutions and are briefly summarized here. These mechanisms differ as to whether [CuCl₂]⁻, Cu⁺, or CuCl are the products of the rate-determining step (RDS)

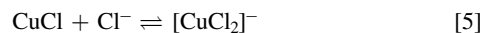
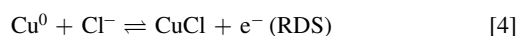
Mechanism 1



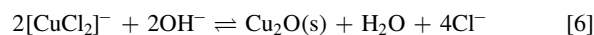
Mechanism 2



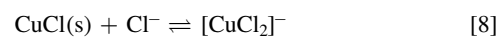
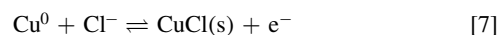
Mechanism 3



However, a serious complication as it pertains to the processing of electronic materials in aqueous solutions is that as the amount of CuCl₂⁻ in the solution increases, solid cuprous oxide is produced



More recently, the anodic dissolution of copper has been investigated in the choline chloride-urea deep eutectic solvent (DES).¹¹ In this case, UV-vis spectroscopy suggests that the copper dissolves in the DES as [CuCl₂]⁻. However, if CuCl is added to the DES beforehand, the formation of a passive film is observed as an intermediate step and is believed to result from this sequence of reactions



The extra CuCl exceeds the solubility of this species in the electrode diffusion layer during the reaction. Modeling of impedance spectroscopy data in these experiments suggests that a porous film of [CuCl₂]⁻ may also be present on the electrode surface.

Room-temperature chloroaluminate ionic liquids (ILs), such as the very popular AlCl₃-1-ethyl-3-methylimidazolium chloride (EtMeImCl) system,¹² offer a unique solvation environment for many metal ions. The use of these ILs for the electrochemical surface finishing of metals was recently reviewed.¹³ These ILs display composition-dependent adjustable Lewis acidity. This acidity depends directly on the relative amounts of the AlCl₃ and organic salt component and is conveniently expressed by the per cent mole fraction (mol %) of AlCl₃ in the mixture. The basic AlCl₃-EtMeImCl IL (< 50 mol % AlCl₃), which contains coordinately unsaturated Cl⁻, provides an ionic solvation environment that is not unlike aqueous NaCl, except without the complications of the H₂O solvent. Thus, the oxidation of Cu⁰ in this composition region of the AlCl₃-EtMeImCl IL would be expected to form species such as [CuCl_p]^{(p-1)-}. In fact, Laher and Hussey¹⁴ studied the solvation and complex formation of Cu⁺ in the basic chloroaluminate IL using potentiometry and absorption spectroscopy. Their results showed that at 40 °C the principal species are most likely [CuCl₂]⁻ and [CuCl₄]³⁻. However, similar work in a related basic room-temperature chloroaluminate system suggested that the latter complex predominated.¹⁵ These results will also be probed again in this study.

*Electrochemical Society Student Member.

**Electrochemical Society Fellow.

^zE-mail: chclh@olemiss.edu

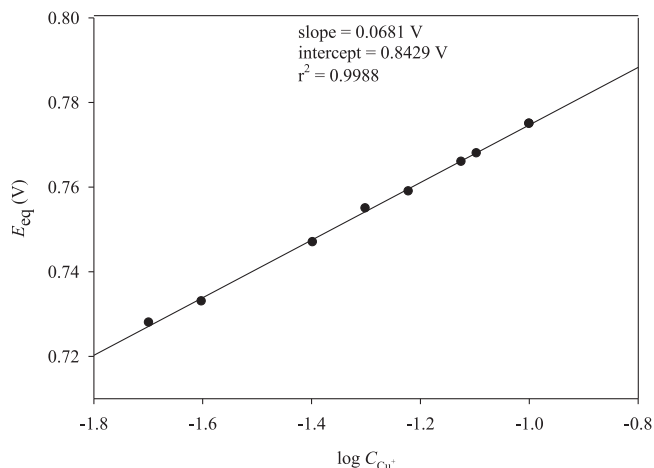


Figure 1. Nernst plot for the $\text{Cu}^+ + \text{e}^- \rightleftharpoons \text{Cu}$ reaction in the 60 m/o AlCl_3 -EtMeImCl ionic liquid.

The Lewis acidic ionic liquid (> 50 mol % AlCl_3) is, however, a very different story. This is because the opposite situation prevails wherein the main ionic component of the solvent is actually a coordinately unsaturated electron deficient species, $[\text{Al}_2\text{Cl}_7]^-$. Thus, there are no “hard” ligands available to form stable anionic complexes with the anodization product. It is presumed that Cu^+ is “solvated” by $[\text{Al}_2\text{Cl}_7]^-$ because once this acidic ion is depleted as the composition reaches 50 mol % AlCl_3 , $\text{CuCl}(\text{s})$ precipitates from the ionic liquid. The anodic dissolution of copper in room-temperature chloroaluminates has not been described and is the focus of this study. Therefore, in this article, we report the mechanism, electron transfer kinetics, and activation energies of copper dissolution as a function of Lewis acidity in the AlCl_3 -EtMeImCl ionic liquid.

Experimental

Electrochemical experiments and the preparation of all ionic liquids were carried out in a nitrogen-filled glove box (LC Technology Solutions, Inc.). The moisture and oxygen levels in the glove box atmosphere were both maintained at less than 1 ppm as determined by the analytical probes supplied by the glove box manufacturer.

Materials.—Aluminum chloride (Fluka > 99 %) was purified by vacuum sublimation from a mixture of AlCl_3 and NaCl as described in a previous article.¹⁶ 1-Ethyl-3-methylimidazolium chloride (EtMeImCl) was purchased in the form of a solid yellow-orange crude product (Sigma-Aldrich, BASF, >95.0 %) and was purified by repeated fractional crystallization until a clear, colorless product was obtained. AlCl_3 -EtMeImCl ILs were prepared by mixing appropriate amounts of aluminum chloride and EtMeImCl in the glove box. The Lewis acidic ILs were conveniently purified by constant current electrolysis (< 2 V applied potential) between two 6 mm diam high-purity aluminum rods (Alfa Aesar, Puritronic® grade) until the final product was water-clear and indicated no electroactive impurities when examined with cyclic staircase voltammetry (CSV). The Lewis basic ILs were prepared by adding the appropriate amount of purified EtMeImCl by weight to electrolyzed 51 mol % AlCl_3 -EtMeImCl.

Electrochemical measurements.—All electrochemical experiments were carried out by using a Biologic SP-200 potentiostat/galvanostat. For rotating disk electrode voltammetry (RDEV) experiments, a Pine Instruments electrode rotator was used to control the electrode rotation rate. Unless indicated otherwise, the temperature of the electrochemical cell was controlled to 33 ± 1 °C with an Ace Glass temperature controller using a homemade furnace

fitted with a platinum resistance thermometer sensor. A three-electrode Pyrex glass cell open to the glove box atmosphere was used for electrochemical experiments. The reference electrode (RE) was an aluminum wire immersed in the 60 mol % AlCl_3 ionic liquid. This electrode was isolated from the bulk IL in a Pyrex tube terminated with an ACE Glass porosity E fritted membrane. Large surface area, multi-coil spirals of either copper or aluminum wire served as the counter electrode (CE), depending on the type of experiment being performed. The working electrode (WE) for copper dissolution kinetic experiments was fabricated by forcing a 5-mm diam copper rod (Alfa Aesar, Puritronic, 99.99 %) into a hollow Teflon cylinder and mounting this on a standard RDE shaft provided by Pine Instruments. The surface area of this electrode is 0.196 cm^2 . The face of the resulting Cu-RDE was polished successively with 400, 600, and 1200 grit silicon carbide sandpaper before use. As material was removed from the Cu-RDE surface during high current dissolution experiments, care was taken to periodically refresh the electrode surface and trim back the protruding Teflon sheath so as not to interfere with convective transport to the electrode surface.

In some cases, it was necessary to prepare solutions containing precise amounts of Cu^+ in the ILs for experiments such as the preparation of Nernst plots. These additions were carried out by the controlled potential anodic dissolution of the large surface area copper wire electrode described above with coulometric monitoring of the charge. These preparation experiments were conducted in a divided cell at applied potentials less than those that could lead to the oxidation of the copper anode directly to Cu^{2+} . In the acidic composition region, the applied potential used to prepare Cu^+ was generally less than 1.5 V,^{15,17} whereas potentials of 0 V or less were employed in the basic ILs.

Results and Discussion

Thermodynamics of the Cu^+/Cu^0 reaction in acidic ionic liquids.—The formal potential, E^0 , of the Cu^+/Cu electrode couple in the IL containing 60 mol % AlCl_3 was estimated by measuring the open circuit potential (OCP), which is equivalent to E_{eq} , at a Cu electrode in the ionic liquid containing different Cu^+ concentrations, C_{Cu^+} . Precise amounts of Cu^+ were added to the IL by using controlled potential electrolysis as described above in the Experimental Section. E^0 (acidic) was estimated from this data by preparing a Nernst plot of E_{eq} vs $\log C_{\text{Cu}^+}$ (Eq. 9), and the result is shown in Fig. 1.

$$E_{\text{eq}} = E^0(\text{acidic}) + 2.303(RT/F) \log C_{\text{Cu}^+} \quad [9]$$

The intercept of this plot gives $E^0 = 0.843$ V, and the slope is 0.068 ± 0.005 V (95% CI). The latter is reasonably close to the expected theoretical value of 0.061 V for a one-electron process at the temperature of these experiments.

Copper anodization kinetics in acidic ionic liquids.—A series of potential steps were carried out to evaluate the current as a function of time at a Cu-RDE using the same method that was used to study Al dissolution in this ionic liquid and in a higher melting alkali halide-based haloaluminate system.^{18,19} Note that the potentials used in these experiments were referenced to the open circuit potential of a freshly prepared Cu^0 electrode immersed in the IL. The potential of this quasi-reference electrode was taken as E_{eq} , so as to provide a reference point for the calculation of the overpotential, $\eta = E_{\text{app}} - E_{\text{eq}}$. Thus, when $\eta > 0$, anodic dissolution of the Cu^0 electrode takes place. Figure 2 shows the current-time plots resulting from these dissolution experiments. A few seconds after applying the potential, the current becomes time independent. In addition, the current increases as the overpotential is made more positive. These plots are functionally similar to those observed for Al dissolution prior to the onset of electrode passivation. However, unlike the previous results for Al, where the formation of a solid film AlCl_3 was

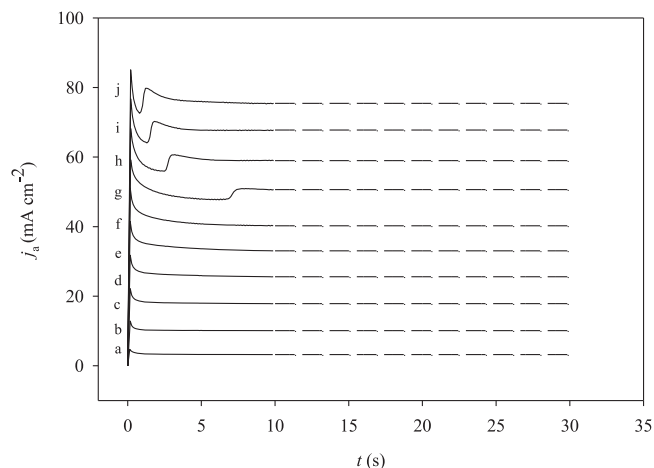


Figure 2. Current-time plots recorded during the anodization of a Cu RDE at different anodic overpotentials in the 60 m/o ionic liquid: (a) 0.039 V, (b) 0.088 V, (c) 0.130 V, (d) 0.172 V, (e) 0.217 V, (f) 0.263 V, (g) 0.285 V, (h) 0.323 V, (i) 0.358 V and (j) 0.400 V. The electrode rotation rate was 157 rad s^{-1} .

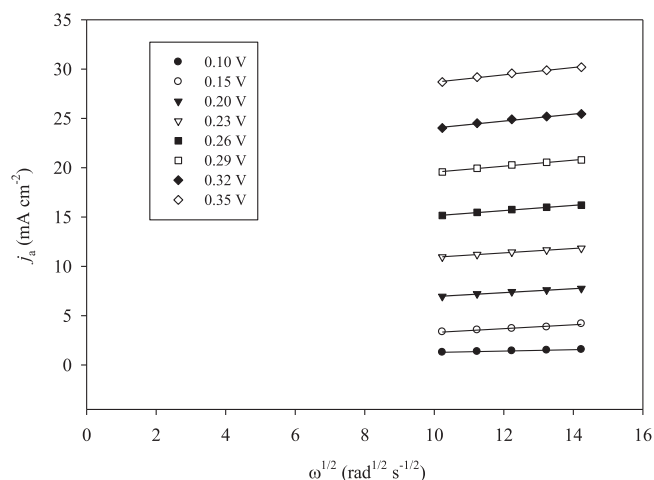


Figure 3. Examples of Levich plots for the anodization of a Cu RDE in the 60 m/o ionic liquid. The anodic overpotentials are shown in the inset.

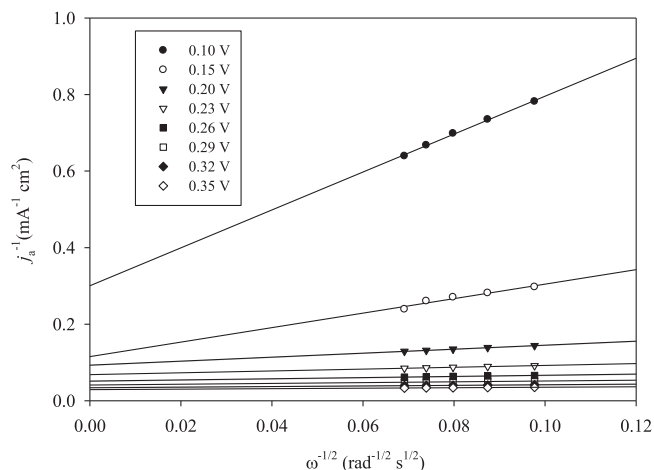


Figure 4. Examples of Koutecky-Levich plots, constructed from the data in Fig. 3: The anodic overpotentials are shown in the inset. The lines are drawn to aid the eye.

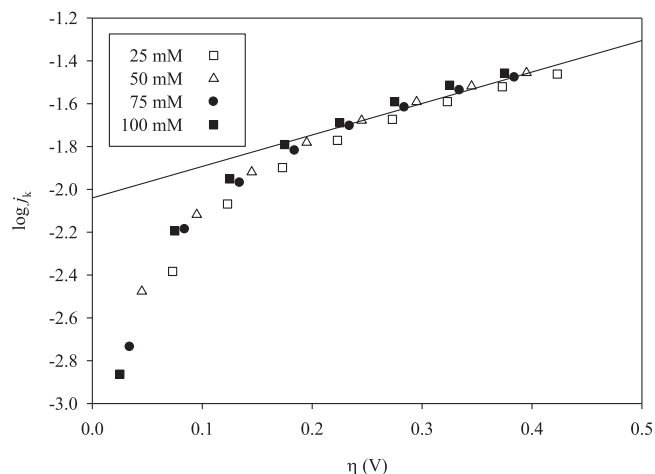


Figure 5. Tafel plots resulting from the Koutecky-Levich analysis of RDE data similar to the example shown in Fig. 4. These RDE data were collected in acidic ionic liquids with added Cu^+ . The Cu^+ concentrations are shown in the inset.

sometimes observed,¹⁹ similar passivation of the copper surface is not evident. However, there are small unexplained minima at short times that are associated with the plots that were recorded at large overpotentials in Figs. 2g–2j, but these minima do not persist. The potential where the oxidation of Cu^+ to Cu^{2+} might be observed in this acidic ionic liquid is estimated to be about 1.8 V.¹⁵ To avoid this complication, we did not attempt any experiments at $\eta > 1.5$.

Levich plots were constructed to evaluate the mass transport of Cu^+ during the anodic dissolution process. The current densities, j_a , were plotted as a function of the square root of the electrode rotation rate, $\omega^{1/2}$. Examples of these plots are shown in Fig. 3. Clearly these plots do not intersect at the origin, and they have very small slopes, suggesting that the reaction is almost completely under kinetic control. This data was then evaluated by using the well-known Koutecky-Levich equation, Eq. 10, for the case of the oxidation of Cu^0 to Cu^+ .²⁰

$$\frac{1}{j} = \frac{1}{F(k_a - k_c C_{\text{Cu}^+})} + [k_c / (k_a - k_c C_{\text{Cu}^+})] [1.613(FD^{2/3})^{-1} \nu^{1/6}] \omega^{-1/2} \quad [10]$$

where k_a and k_c are the potential-dependent anodic and cathodic rate constants, and all other symbols have their usual meaning. In this equation, the intercept, $1/F(k_a - k_c C_{\text{Cu}^+})$ corresponds to $1/j_k$, where j_k corresponds to the current density at infinite rotation rate. Equation 10 simplifies considerably when Cu^+ is absent from the bulk solution and/or when large anodic overpotentials are employed, such that $k_a \gg k_c C_{\text{Cu}^+}$. Examples of these graphs are shown in Fig. 4.

In order to assess the relationship between the kinetic current and the concentration of Cu^+ , numerous RDE anodization measurements were used to collect data in ionic liquid solutions with different Cu^+ concentrations and then plotted according to the Tafel equation

$$\log j_k = \log j_0 + a_a \eta F / (2.303RT) \quad [11]$$

where j_0 and α_a are the exchange current density and anodic transfer coefficient, respectively.²¹ Tafel plots for each Cu^+ concentration that are based on j_k taken from the corresponding Koutecky-Levich plots are collected in Fig. 5. These Tafel plots display the classic shape, including a non-linear segment corresponding to the influence of the back reaction and a linear segment at higher overpotentials, $\eta \gg RT/nF$, where the back reaction is negligible. A single straight line was fitted to the pooled data in the linear segments of these plots and is shown in Fig. 5. This result strongly suggests that the reaction order, $(\partial \log j_0 / \partial C_{\text{Cu}^+})_{T,P}$,²² for the anodization of Cu^0 , is zero with respect to C_{Cu^+} . That is, Cu^+ does not participate in the RDS of the

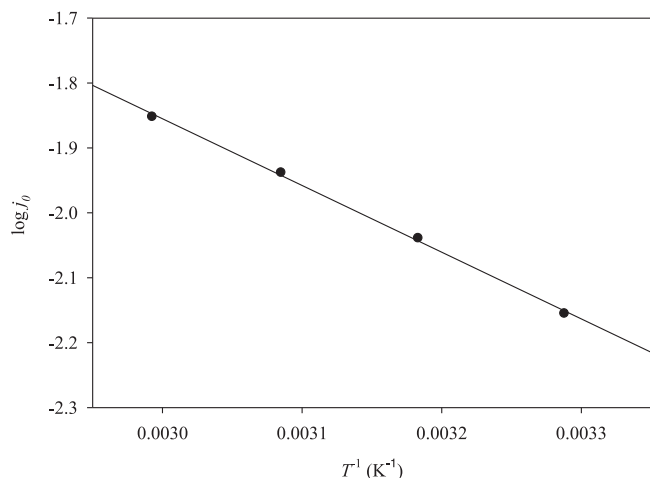


Figure 6. Arrhenius plot of $\log j_0$ vs $1/T$ for data collected at 31 °C, 41 °C, 51 °C and 61 °C.

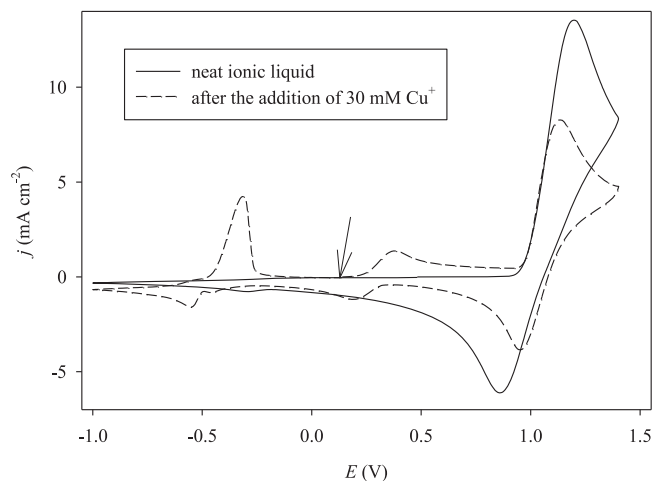


Figure 7. Cyclic staircase voltammograms recorded at a stationary platinum electrode in the 48 m/o $\text{AlCl}_3\text{-EtMeImCl}$ ionic liquid before and after the addition of 30 mM Cu^+ . The scan rate was 50 mV s^{-1} .

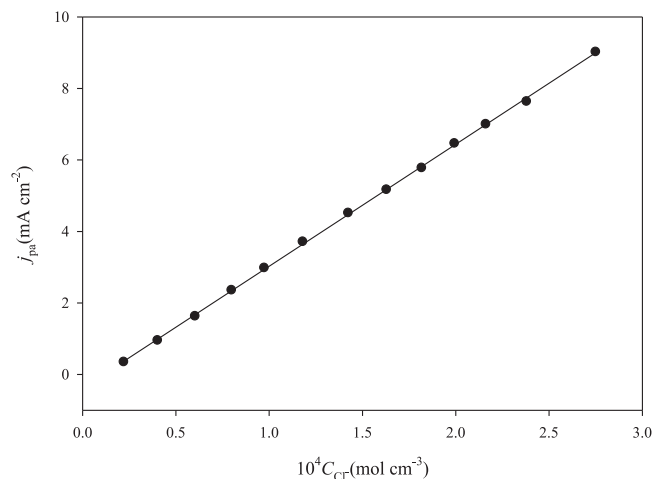


Figure 8. Chloride concentration calibration curve prepared from the CSV peak current for the oxidation of Cl^- in the basic ionic liquid at 33 ± 1 °C.

dissolution reaction. For the pooled data in Fig. 5, the values of j_0 and α_a , are 7.00 mA cm^{-2} and 0.054, respectively. Surprisingly, this diminutive value of $\alpha_a \sim 0$ is not unusual and has been observed

during previous investigations involving the anodic dissolution of Cu^0 .^{20,25}

The apparent activation free energy, $\Delta G_{a,0}^\#$, for this anodic reaction can be estimated by determining j_0 at several additional temperatures. Because the expensive Pine Instrument Teflon-sheathed Cu RDE might be damaged above ~ 60 °C, only a small temperature range could be sampled with this electrode. The experimental data were very similar to those obtained at 33 °C, and for reasons of space and repetition, the Tafel plots are not reproduced here. A plot of $\log j_0$ vs $1/T$ that was constructed from this data is shown in Fig. 6. The data points were recorded at 31 °C, 41 °C, 51 °C and 61 °C. $\Delta G_{a,0}^\#$ was estimated from the slope of this plot with Eq. 12.

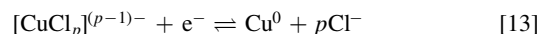
$$\Delta G_{a,0}^\# = -2.303R[\partial \log j_0 / \partial (1/T)] \quad [12]$$

The resulting value of $\Delta G_{a,0}^\#$ is 19.7 kJ mol^{-1} .

Thermodynamics of the Cu^+/Cu^0 reaction in basic ionic liquids.

—The experiments described below were carried out in basic ionic liquids that contained very small amounts of free Cl^- . Thus, a convenient method was needed to monitor the chloride concentration during these experiments. Figure 7 shows cyclic staircase voltammograms recorded in the Lewis basic 48 m/o $\text{AlCl}_3\text{-EtMeImCl}$, before and after the addition of electrogenerated Cu^+ . The prominent oxidation wave at ~ 1.2 V, which is due to the two-electron oxidation of Cl^- ,²³ is clearly visible in the voltammogram recorded before the addition of Cu^+ . Standard calibration curves were prepared by recording the peak current for this oxidation wave, j_{pa} , at a fixed scan rate and temperature in solutions with known Cl^- concentrations, C_{Cl^-} . An example of a calibration curve is shown in Fig. 8. We have used this analytical procedure for determining C_{Cl^-} in other investigations with great success.^{24–26} The voltammogram of this solution in Fig. 7 recorded after the addition of Cu^+ shows a wave at $E_p^a = 0.38$ V corresponding to the oxidation of Cu^+ to Cu^{2+} and a reduction wave at $E_p^c \sim -0.6$ V arising from the reduction of Cu^+ to Cu^0 .¹⁵ Because this investigation will only focus on the anodization of Cu^0 to Cu^+ , as was the case in the acidic composition of the ionic liquid (vide supra), no experiments were performed at applied potentials more positive than 0 V (or $\eta = 0.50$ V) to avoid complications due to the oxidation of Cu^+ to Cu^{2+} . A large surface area aluminum wire counter electrode, which was open to the bulk solution, was used during these experiments in order to reduce any Cu^+ generated during the anode reaction. Thus, these experiments were conducted without Cu^+ in the bulk solution.

Determination of $E^{0'}$ for the Cu^+/Cu reaction in the basic ionic liquids was more complex than in the case of the acidic composition of the IL because Cl^- is a participant in the electrode reaction, and therefore, its concentration must be considered in the Nernst equation. Thus, it can be envisioned that Cu^+ in the basic ionic liquid is complexed by Cl^- as one or more species having the general formula, $[\text{CuCl}_p]^{(p-1)-}$,¹⁴ and that the Cu^0 reaction, written here as a reduction, would be



The corresponding Nernst equation is then

$$E_{\text{eq}} = E^{0'}(\text{basic}) - 2.303(RT/F) \log (C_{\text{Cl}^-})^p + 2.303(RT/F) \log C_{[\text{CuCl}_p]^{(p-1)-}} \quad [14]$$

where $C_{[\text{CuCl}_p]^{(p-1)-}}$ is the total bulk concentration of the complexed Cu^+ species. (The free energy for the complexation of Cu^+ by Cl^- is very negative, and thus all of the added Cu^+ is assumed to be complexed by Cl^- when the latter is in large excess.¹⁴) Two different Nernst plots were prepared in order to determine $E^{0'}(\text{basic})$ and to probe the identity of $[\text{CuCl}_p]^{(p-1)-}$. In the first type of experiment, a Nernst plot was prepared by measuring E_{eq} as

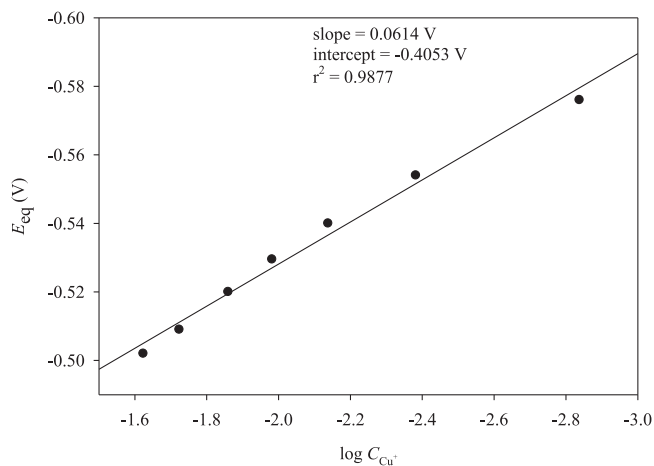


Figure 9. Nernst plot for the $\text{Cu}^+ + \text{e}^- \rightleftharpoons \text{Cu}$ reaction recorded in the basic $\text{AlCl}_3\text{-EtMeImCl}$ ionic liquid containing 675 mM free Cl^- .

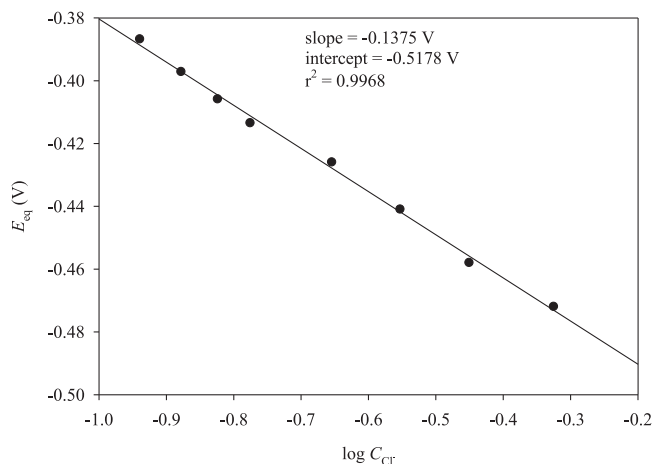


Figure 10. Equilibrium potential of the Cu^+/Cu reaction as a function of the Cl^- concentration in the basic $\text{AlCl}_3\text{-EtMeImCl}$ ionic liquid.

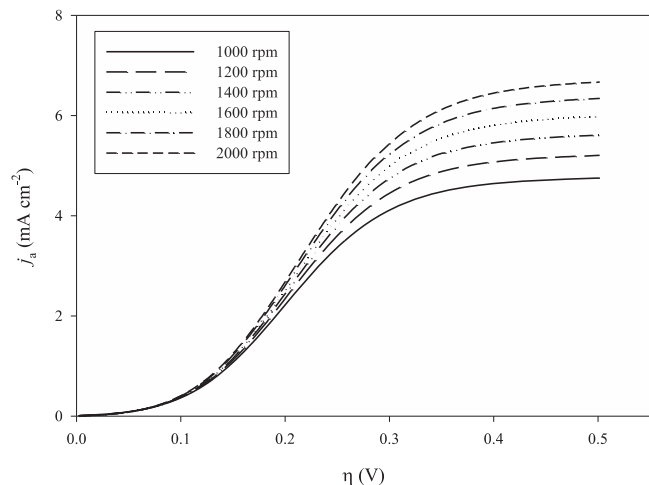


Figure 11. Voltammograms showing the anodization of a Cu RDE at different rotation rates in basic $\text{AlCl}_3\text{-EtMeImCl}$ containing 156 mM free Cl^- .

a function of $\log C_{[\text{CuCl}_p]^{(p-1)-}}$ at a copper electrode in the basic IL containing a large excess of Cl^- . This plot (Fig. 9) is reasonably linear with a slope of 0.061 ± 0.006 V (95% CI) and an intercept of

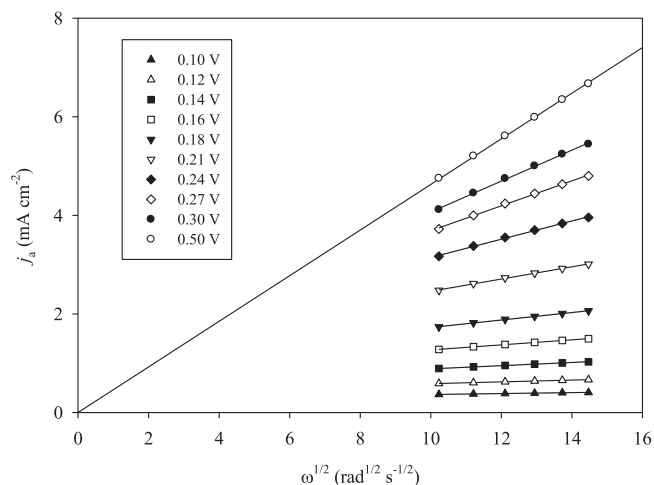


Figure 12. Levich plots prepared from the data in Fig. 11. The anodic overpotentials were: (▲) 0.10 V, (△) 0.12 V, (■) 0.14 V, (□) 0.16 V, (▼) 0.18 V, (▽) 0.21 V, (◆) 0.24 V, (◇) 0.27 V, (●) 0.30 V, (○) 0.50 V (at limiting current).

-0.405 ± 0.013 V. The former is in excellent agreement with the 0.061 V slope expected for a one-electron reaction at the temperature of these experiments. A second Nernst plot was constructed by measuring E_{eq} at a copper electrode in the Lewis basic IL in which $C_{[\text{CuCl}_p]^{(p-1)-}}$ was fixed and C_{Cl^-} was varied. The resulting plot of E_{eq} vs $\log C_{\text{Cl}^-}$ is shown in Fig. 10. The slope of this plot is -0.138 ± 0.006 V with an intercept of -0.518 ± 0.004 V. This slope corresponds to a value of $p = 2.3 \pm 0.1$, strongly suggesting that the predominant product of the anodization of Cu^0 in the basic IL in the range of chloride concentration investigated is $[\text{CuCl}_2]^-$.

Using a value of $p = 2$ and inserting the appropriate values of $C_{[\text{CuCl}_p]^{(p-1)-}}$, C_{Cl^-} , and the intercepts of the plots shown in Figs. 9 and 10 into Eq. 14 gave $E^0(\text{basic}) = -0.426$ V and -0.398 V, respectively. These values are in reasonably good agreement given the difference in experimental approaches used to obtain the estimates of E^0 . The corresponding value determined in the acidic IL (vide supra) is $E^0(\text{acidic}) = 0.843$ V and is significantly more positive against the identical reference electrode employed in the basic IL. This large difference in the formal potentials clearly confirms that Cu^+ is only weakly complexed or solvated in the acidic IL and strongly complexed by Cl^- in the basic IL. Using the value for $E^0(\text{acidic})$ and the average of the two values of $E^0(\text{basic})$, -0.412 V, the free energy of formation for $[\text{CuCl}_2]^-$, $\Delta G_f^\circ[\text{CuCl}_2]^- = -121$ kJ mol $^{-1}$. The formation constant for the reaction between Cu^+ and Cl^- to produce $[\text{CuCl}_2]^-$ is then $K^f = 4.7 \times 10^{20}$, illustrating the extraordinary stability of this complex in the basic IL.

Copper anodization kinetics in basic ionic liquids.—To investigate Cu^0 oxidation in basic ionic liquids with RDE voltammetry, experiments were performed over a range of rotation rates from 1000 to 2000 rpm. Examples of such voltammograms are shown in Fig. 11. Unlike those experiments that were carried out in the acidic IL where the current simply increases with η until the oxidation of Cu^0 to Cu^{2+} is observed, when η is increased to ~ 0.36 V in the basic IL, a well-defined limiting current is observed. Levich plots constructed from the data in Fig. 11 at different rotation rates are given in Fig. 12, and they show that the oxidation of Cu^0 to Cu^+ transitions from mixed control at η below 0.36 V to convective mass-transport control as η is increased.

In order to probe the relationship between the RDE voltammetry current for the Cu^0 oxidation reaction and the Cl^- concentration, experiments were carried out similar to those shown in Fig. 11, but in ILs containing from 77 to 555 mM Cl^- . In this case, the limiting current measured at $\eta > 0.36$ V, $j_{l,a}$, was analyzed by plotting the viscosity corrected limiting current, $j_{l,a}'$, at a fixed value of ω vs

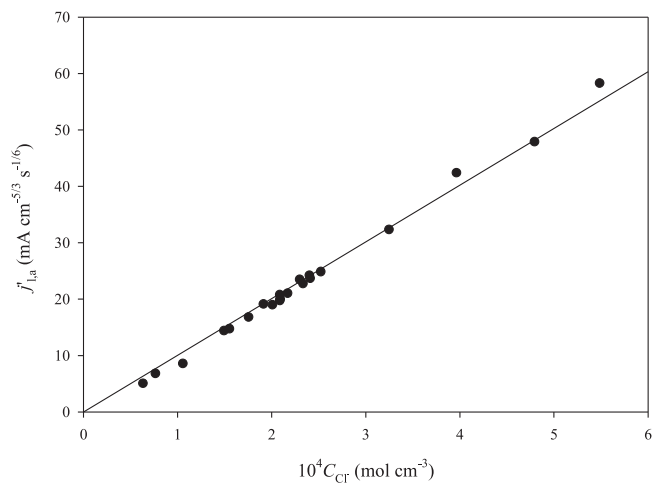


Figure 13. Viscosity-corrected limiting current densities vs the free Cl^- concentration in the basic $\text{AlCl}_3\text{-EtMImCl}$. In each case, the electrode rotation rate was 188 rad s^{-1} .

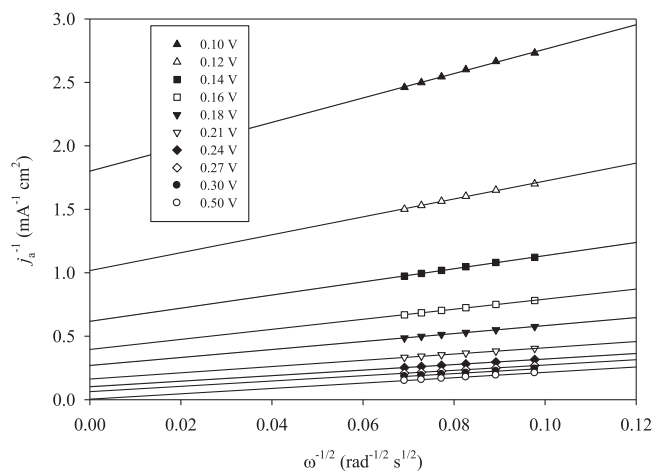


Figure 14. Examples of Koutecky-Levich plots, constructed from the data in Fig. 12. The anodic overpotentials were the same as those given in the previous figure. The lines are drawn to aid the eye.

$C_{\text{Cl}^-}^{-19.27}$

$$j_{l,a}' = j_{l,a} \nu^{1/6} = 0.62FD^{2/3} \omega^{1/2} C_{\text{Cl}^-} \quad [15]$$

In this expression, ν , is the kinematic viscosity of the ionic liquid, which is calculated from data given in the article by Fannin, et al.²⁸ All other symbols have their usual meaning. The resulting plot is shown in Fig. 13. Clearly, under these conditions, the oxidation of Cu^0 is directly dependent on the mass transport of Cl^- to the electrode surface.

The oxidation of copper as a function of C_{Cl^-} was also probed in these same nine solutions at smaller overpotentials, where mixed control is observed. The Levich plots that were prepared from the current vs rotation rate data recorded at each overpotential were similar to the examples shown in Fig. 12. The data in these plots were used to construct Koutecky-Levich plots and were similar in appearance to those given in Fig. 14. As noted above in the acidic IL, the intercepts of these plots correspond to $1/j_k$. Figure 15 illustrates Tafel plots that were prepared by plotting $\log j_k$ vs η for the data obtained at each C_{Cl^-} . The linear portions of these Tafel plots were extrapolated to $\eta = 0$ to obtain j_0 , and the slopes of these plots were used to estimate $\alpha_a = 0.37 \pm 0.04$. Because j_0 shows a clear dependence on C_{Cl^-} , the order of the microscopic reaction for the oxidation of Cu^0 can be determined from the expression²²

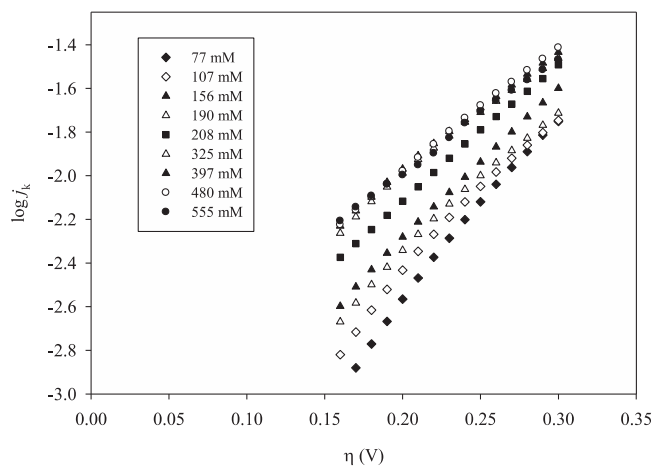


Figure 15. Tafel plots constructed from RDE voltammetry experiments recorded at different Cl^- concentrations similar to the experiments shown in Fig. 11.

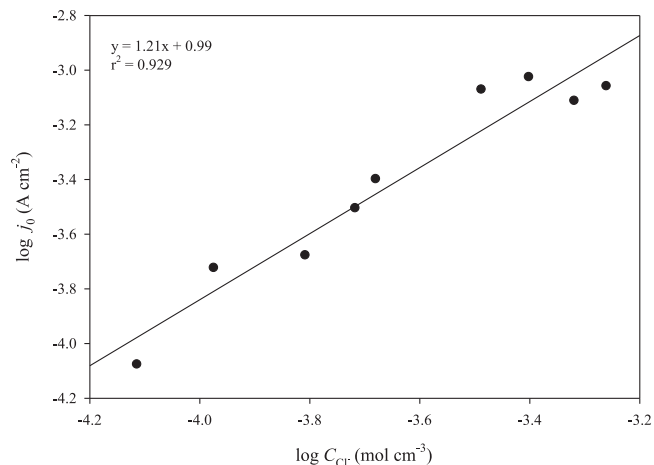


Figure 16. Log-log plot of the exchange current density, j_0 , vs the Cl^- concentration constructed from the data in Fig. 15.

$$\rho = (\partial \log j_0 / \partial \log C_{\text{Cl}^-})_{h,T,P} \quad [16]$$

A plot of $\log j_0$ vs $\log C_{\text{Cl}^-}$ is shown in Fig. 16, and the slope of this plot is $\sim 1.2 \pm 0.3$. This clearly suggests that at small overpotentials the dissolution reaction is first order with respect to Cl^- , indicating that the mechanism for the oxidation of Cu^0 in the basic IL prior to the onset of mass transport control follows the pathway represented by Eqs. 4 and 5 where a single Cl^- is involved in the RDS.

Conclusions

In the Lewis acidic $\text{AlCl}_3\text{-EtMImCl}$ ionic liquid, the anodic dissolution of Cu proceeds under mixed kinetic-mass transport control. No limiting oxidation current was observed in the accessible potential region of the acidic ionic liquid prior to the potential at which Cu^+ is converted to Cu^{2+} . The value of j_0 was 7.00 mA cm^{-2} at 306 K with $\Delta G_{a,0}^\ddagger = 19.7 \text{ kJ mol}^{-1}$ and was independent of the Cu^+ concentration. This is larger than the 17.3 kJ mol^{-1} found during the oxidation of Al in this same IL,¹⁹ but close to the activation energy of 19.1 kJ mol^{-1} observed for the anodic dissolution of Cu^0 in the choline chloride-urea DES by Tang et al.¹¹ Most importantly, the magnitude of the oxidation current observed in the Lewis acidic IL is comparable to that observed in aqueous Cl^- solutions.²⁹

On the other hand, the anodic dissolution of Cu^0 in the Lewis basic IL containing unbound Cl^- gives an entirely different result. Potentiometric measurements clearly indicate that the oxidation product is $[\text{CuCl}_2]^-$. At small positive overpotentials, the anodization process in this IL exhibits mixed control. Tafel analysis at different C_{Cl^-} indicated that only a single Cl^- is involved in the RDS. This supports the mechanism represented by Eqs. 4 and 5 proposed by Lee and Nobe²⁹ in aqueous chloride solutions when $C_{\text{Cl}^-} < 1 \text{ M}$. At more positive overpotentials, a well-defined limiting current is observed that scales linearly with the Cl^- concentration. However, even under these limiting current conditions, the anodic current observed in the more viscous basic IL is approximately one order of magnitude less than found in the acidic IL. It should also be noted that passivation of the copper surface during anodic dissolution was not observed in either composition region of the IL, suggesting that the oxidation of Cu^0 in the acidic and basic $\text{AlCl}_3\text{-EtMeImCl}$ ionic liquids is considerably simpler than found in aqueous NaCl solutions. The results of this investigation indicate that both ILs may have value for the surface treatment of Cu^0 .

ORCID

Charles L. Hussey  <https://orcid.org/0000-0002-3954-8204>

References

1. M. C. Bastos, M. H. Mendonca, M. M. M. Neto, L. Proenca, and I. T. E. Fonseca, *J. Appl. Electrochem.*, **38**, 627 (2008).
2. M. Datta, *Electrochim. Acta*, **48**, 2975 (2003).
3. T. Ritzdorf, *ECS Trans.*, **6**, 1 (2007).
4. Y.-J. Oh, G.-S. Park, and C.-H. Chung, *J. Electrochem. Soc.*, **153**, G617 (2006).
5. S. Sato et al., *Tech. Dig. Int. Electron Devices Meet.*, **2000**, 80 (2001).
6. J. McAndrew, R. Solanki, and J. Huo, *J. Mater. Eng. Perform.*, **13**, 413 (2004).
7. G. D. Kwon, Y. W. Kim, E. Moyan, D. H. Keum, Y. H. Lee, S. Baik, and D. Probat, *Appl. Surf. Sci.*, **307**, 731 (2014).
8. J. Huo, R. Solanki, and J. McAndrew, *J. Mater. Eng. and Perform.*, **13**, 413 (2004).
9. M. El-Batouti, *Ant-Corros. Meth. and Mater.*, **43**, 27 (1996).
10. G. Kear, B. D. Barker, and F. C. Walsh, *Corros. Sci.*, **46**, 109 (2004).
11. J. Tang, C. Xu, X. Zhu, H. Liu, X. Wang, M. Huang, Y. Hua, Q. Zhang, and Y. Li, *J. Electrochem. Soc.*, **165**, E406 (2018).
12. J. S. Wilkes, J. A. Levisky, R. A. Wilson, and C. L. Hussey, *Inorg. Chem.*, **21**, 1263 (1982).
13. T. Tsuda, G. R. Stafford, and C. L. Hussey, *J. Electrochem. Soc.*, **164**, H5007 (2017).
14. T. M. Laher and C. L. Hussey, *Inorg. Chem.*, **22**, 3247 (1983).
15. C. Nanjundiah and R. A. Osteryoung, *J. Electrochem. Soc.*, **130**, 1312 (1983).
16. S. K. Strubinger, I.-W. Sun, W. E. Cleland, and C. L. Hussey, *Inorg. Chem.*, **29**, 4246 (1990).
17. C. L. Hussey, L. A. King, and R. A. Carpio, *J. Electrochem. Soc.*, **126**, 1029 (1979).
18. C. Wang and C. L. Hussey, *J. Electrochem. Soc.*, **162**, H151 (2015).
19. C. Wang and C. L. Hussey, *J. Electrochem. Soc.*, **163**, H1186 (2015).
20. S. R. de Sanchez and D. J. Schiffrin, *Corros. Sci.*, **22**, 585 (1982).
21. R. Guidelli, R. G. Compton, J. M. Feliu, E. Gileadi, J. Lipkowski, W. Schmickler, and S. Trasatti, *Pure Appl. Chem.*, **86**, 245 (2014).
22. E. Gileadi, *Electrode Kinetics for Chemists, Chemical Engineers, and Materials Scientists* (VCH, New York) p. 597 (1993).
23. L. Aldous, D. S. Silvester, C. Villagran, W. R. Pitner, R. G. Compton, M. C. Lagunas, and C. Hardacre, *New J. Chem.*, **30**, 1576 (2006).
24. L.-H. Chou, W. E. Cleland, and C. L. Hussey, *Inorg. Chem.*, **51**, 11450 (2012).
25. L.-H. Chou and C. L. Hussey, *Inorg. Chem.*, **53**, 5750 (2014).
26. Y. Pan and C. L. Hussey, *Inorg. Chem.*, **52**, 3241 (2013).
27. M. Datta and D. Verduyn, *J. Electrochem. Soc.*, **137**, 3016 (1990).
28. A. A. Fannin, D. A. Floreani, L. A. King, J. S. Landers, B. J. Piersma, D. J. Stech, R. L. Vaughn, J. S. Wilkes, and J. L. Williams, *J. Phys. Chem.*, **88**, 2614 (1984).
29. H. P. Lee and K. Nobe, *J. Electrochem. Soc.*, **133**, 2035 (1986).